

Suppression of nuclear polarization near the surface of optically pumped GaAs

M. R. Fitzsimmons,¹ B. J. Kirby,^{1,*} N. W. Hengartner,¹ F. Trouw,¹ M. J. Erickson,² S. D. Flexner,² T. Kondo,^{2,†} C. Adelmann,² C. J. Palmström,² P. A. Crowell,² W. C. Chen,³ T. R. Gentile,³ J. A. Borchers,³ C. F. Majkrzak,³ and R. Pynn⁴

¹Los Alamos National Laboratory, Los Alamos, New Mexico 87545, USA

²University of Minnesota, Minneapolis, Minnesota 55455, USA

³National Institute of Standards and Technology, Gaithersburg, Maryland 20899, USA

⁴Physics Department, University of Indiana, Bloomington, Indiana 47405, USA

(Received 21 August 2007; revised manuscript received 12 October 2007; published 3 December 2007)

We measured the spin dependence of polarized neutrons reflected by a GaAs sample as it was optically pumped. This dependence was correlated with the helicity of the circularly polarized light and found to oscillate with neutron wave vector transfer. The data provide definitive evidence that optically induced nuclear polarization in GaAs is not uniform with depth. Quantitative analysis of the data shows that nuclear polarization is suppressed for tens of nanometers near the surface of GaAs.

DOI: [10.1103/PhysRevB.76.245301](https://doi.org/10.1103/PhysRevB.76.245301)

PACS number(s): 72.25.Fe, 21.10.Ky, 61.12.Ha, 76.70.Fz

I. INTRODUCTION

Proposed applications of spin-polarized transport, such as the spin-field-effect transistor,¹ require populations of spin-polarized electrons and precise control of their spin-dynamics and relaxation. In zinc-blende semiconductors such as GaAs, nonequilibrium populations of spin-polarized electrons can be optically^{2,3} or electronically^{4,5} produced. Electron spin lifetimes in GaAs can be long⁶ enough to allow magnetic fields of a few Gauss to influence electron spin dynamics. Since effective magnetic fields due to the hyperfine interaction between the electron and nuclear spin systems can be thousands of Gauss, such fields can profoundly affect electron spin lifetimes. The interaction strength is strongest when spin-polarized carriers are localized, for example, in quantum wells⁷ or at donor sites.⁸ Since the electron density and spin polarization can vary rapidly due to quantum confinement, doping profile, or to the presence of interfaces, the nuclear polarization and resulting effective hyperfine field may be nonuniform.⁹ Thus, an independent means of determining the spatial distribution of nuclear polarization is desirable in order to better understand the effects of hyperfine interactions in semiconductors.

We report results of neutron scattering and luminescence studies of nuclear polarization in heavily doped GaAs. The luminescence studies led us to anticipate a moderately strong dependence of neutron beam polarization with nuclear polarization, *provided that the nuclear polarization is uniformly distributed*. However, the observed dependence is very weak. The dramatic discrepancy is due to the difference between the sensitivities of luminescence and polarized neutron reflectometry (PNR)^{10–12} to the nuclear polarization in the bulk and near the sample's surface. PNR measures the variation of the nuclear polarization with nanometer-depth resolution in the sample averaged over its *lateral* dimensions.^{10–12} The PNR signal is strongest when sharp planar interfaces separate layers with different (spin-dependent) nuclear scattering length densities, as would be the case for a uniformly polarized sample in air. However, since the nuclear polarization is nonuniform with depth (as will be shown later) in GaAs, the size of the neutron signal is much less than anticipated. In

contrast, luminescence is observed from a relatively large *volume* of material extending to depths of order 1 μm .¹³ Over this length scale, the nuclear polarization is relatively uniform.

II. LUMINESCENCE RESULTS

We examined two samples with PNR. Sample A consisted of a 1 μm thick epilayer of compensated *p*-type GaAs, grown on a semi-insulating GaAs substrate using molecular beam epitaxy. The epilayer was codoped with Be ($2 \times 10^{18} \text{ cm}^{-3}$) and Si ($6 \times 10^{17} \text{ cm}^{-3}$). This design was chosen to enhance the efficiency of dynamic nuclear polarization (DNP)⁸ and for the ease with which the hyperfine field¹⁴ B_N induced by DNP could be measured from polarized photoluminescence.¹⁵ The rapid recombination of photoelectrons in compensated *p*-type GaAs maintains a high average electron spin polarization under optical pumping.⁸ This fact, in combination with the large number of electrons localized on donor sites, leads to efficient DNP. In contrast, sample B did not contain any acceptors, leading to a small electron spin polarization at the optical power densities used in our experiment. Consequently, the nuclear polarization should be small in sample B.

B_N in Sample A was measured using the optical Hanle effect,^{16,17} which is sensitive to the precession and dephasing of spin-polarized photoelectrons in a transverse magnetic field. The sample was mounted in a magneto-optical cryostat in which a field \vec{B}_A was applied at an angle $\alpha \sim 75^\circ$ from the sample's surface normal. The sample was illuminated with circularly polarized light (CPL) (wavelength=805 nm).

Photoluminescence was collected using a polarizer and variable wave plate, which could be set to detect either “right” (*r*) or “left” (*l*) CPL, as a function of field. The polarization of the luminescence $P_{lum} = (I_r - I_l) / (I_r + I_l)$ was calculated from the integrals I_r and I_l of the spectra collected for the two settings of the wave plate. Hanle curves were obtained by measuring P_{lum} as a function of B_A (Fig. 1). The broad peaks near $\pm 0.2 \text{ T}$ occur when $B_A + B_N = 0$ —a condition that suppresses precession of the electron polarization,

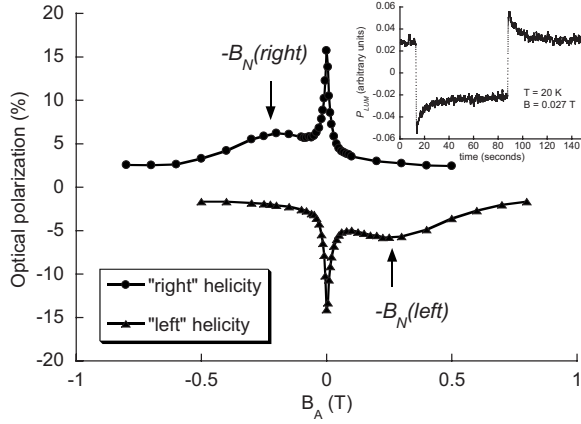


FIG. 1. Hanle curves used to obtain B_N . The two curves were obtained for different helicities of the incident light, corresponding to different directions of the optically pumped electron spin polarization. Inset: the time dependence of the optical polarization after subsequent reversals of the wave plate from right to left.

thus maximizing P_{lum} . The position of this maximum is, therefore, a measurement of B_N . B_N and thus the nuclear polarization P_N are reversed by changing the helicity of the incident light polarization (Fig. 1), i.e., $P_N(\text{"right"}) = -P_N(\text{"left"})$. Hanle curves were also measured as functions of angle α , power density, and sample temperature. B_N increases slowly with decreasing α and saturates at power densities above $\rho = 0.1 \text{ W/cm}^2$, provided that the sample temperature is $T \leq 30 \text{ K}$. For $\alpha = 75^\circ$, $\rho = 0.1 \text{ W/cm}^2$, and $T = 20 \text{ K}$, we obtained $P_N = 4\% \pm 1\%$ for sample A from the measured value of B_N .¹⁸

In addition to the field dependence data shown in Fig. 1, we also measured the characteristic time for P_{lum} to equilibrate when the orientation of the electron spin polarization was reversed (achieved by rapidly switching the orientation of the wave plate). At high temperatures (above 70 K), the response appeared instantaneous (limited by the measurement time of 100 ms). At low temperatures, P_{lum} responded on a time scale of several seconds due to the slow relaxation of nuclear spins. The response observed at 20 K in an applied field of 265 G is shown in the inset of Fig. 1. Although the relaxation of the signal cannot be described by a single time constant, we estimate bounds on the nuclear spin relaxation time T_1 between 1 and 10 s (appropriate for the temperature and field used in the neutron scattering experiment). Note that the field-dependent Hanle data (main panel of Fig. 1) were taken with a waiting time of order 20 s between data points, so that the nuclear spin polarization was completely equilibrated prior to measurement.

III. NEUTRON SCATTERING RESULTS

For the PNR experiment, samples (area $\sim 2 \text{ cm}^2$) were cooled to 20 K in a He vapor cryostat. A sample could be rotated about the y axis inside the cryostat (Fig. 2) such that the sample's surface normal was parallel to the incident laser light (i.e., $\alpha = 0$), independent of the alignment of the sample with respect to the neutron beam. CPL (polarization

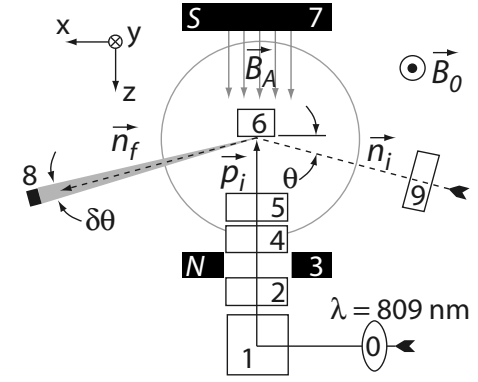


FIG. 2. Diagram of the neutron experiment. Neutron (dashed line) and light beams (solid line), (0) lens, (1) polarizing beam splitter, (2) wave plate, (3) and (7) magnets, (4) and (5) windows, (6) sample, (8) neutron detector pixel, and (9) flipper are shown. The field applied to the sample B_A and that outside the cryostat B_0 are shown. The incident light wave vector (with wavelength $\lambda = 809 \text{ nm}$) is shown as \vec{p}_i . The incident and final (reflected) neutron wave vectors are shown as \vec{n}_i and \vec{n}_f , respectively.

$= 99.7\% \pm 0.6\%$; wavelength = 809 nm) entered the cryostat through a pair of fused silica windows. The incident power density on the sample was 0.25 W/cm^2 . A magnetic field $B_A = 265 \pm 15 \text{ G}$ was applied to the sample along its surface normal by permanent magnets. One of the magnets had a 3.2 cm diameter hole to transmit light.

A polarized neutron beam (polarization between 93% and 96%) was incident on the sample at the angle $\theta = 0.53^\circ$ (Fig. 2) with respect to the sample's surface. Outside the cryostat, the neutron beam polarization was parallel to the $\sim 50 \text{ G}$ field \vec{B}_0 . Near the cryostat's outer surface, $|\vec{B}_0|$ decreased and $|\vec{B}_A|$ increased so the net field induced a $\pi/2$ adiabatic rotation of the neutron beam polarization so that the polarization was parallel (or antiparallel) to \vec{B}_A at the sample.

The neutron wavelength λ_n ranging from 4 to 12 Å was measured using time-of-flight techniques with a precision $\delta\lambda/\lambda_n < 0.5\%$. The wave vector transfer \vec{Q} ($Q = 4\pi \sin \theta / \lambda_n$) is the difference between the incident neutron wave vector \vec{n}_i and the wave vector of the specularly reflected beam \vec{n}_f (Fig. 2). The intensity of the reflected neutron beam normalized to that of the incident beam for neutron beam polarization parallel (+) and antiparallel (−) to the net nuclear spin of GaAs yielded the reflectivities $R^\pm(Q)$. The polarization of the neutron beam was reversed (relative to \vec{B}_A for fixed light polarization) at the 20 Hz frequency of the neutron source using a Mezei π spin flipper.^{19,20} By reversing the polarization of the neutron beam over a short time scale, instrumental bias for one neutron spin state over the other can be reduced during the two-week-long measurement (for each sample).

The intensity and position of the reflected neutron beam were measured by a linear position sensitive neutron detector. Each detector pixel integrated the intensity of the neutron beam over scattering angles ranging $\pm \delta\theta/2$ ($= \pm 0.015^\circ$) about a nominal scattering angle 2θ . The diffuse scattering underneath the specular reflectivity was estimated from mea-

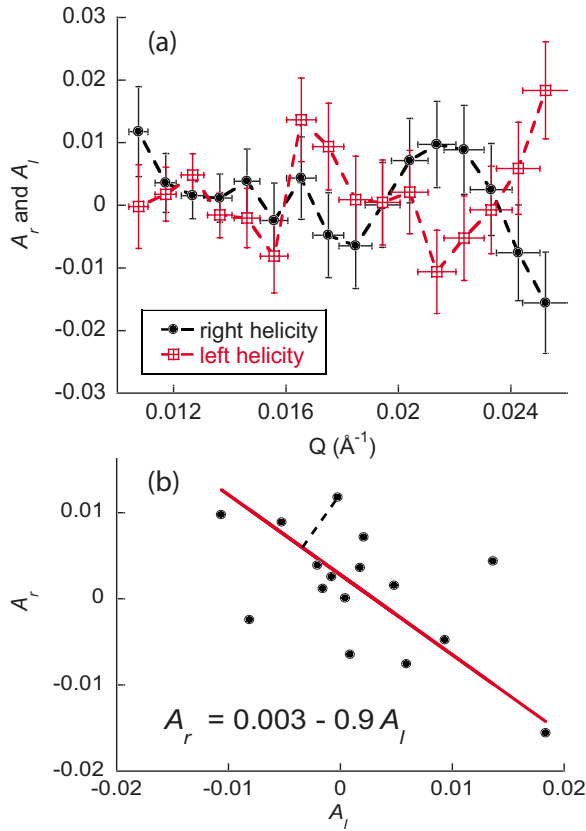


FIG. 3. (Color online) Neutron spin asymmetry is shown as a function of neutron wave vector transfer for (a) right and left CPL. (b) Principal component analysis showing A_r and A_l . Additional data for this sample and sample B are in Ref. 21.

measurements of the scattering $\pm 0.1^\circ$ away from the specular reflectivity. The diffuse scattering was not spin dependent, and the same estimate was subtracted from the data for both neutron spin states to obtain R^\pm .²¹

R^+ and R^- are given by the same function of the appropriate neutron-spin-dependent scattering length: $b_c \pm [I/(2I+1)]\Delta b P_N(z)$. $b_c = 1.387 \times 10^{-4} \text{ \AA}$ ($\Delta b = -3.17 \times 10^{-5} \text{ \AA}$) is the spin independent (dependent) part of the coherent spin neutron scattering length for GaAs.²² $I=3/2$ is the nuclear spin of Ga and As. z represents the depth into the sample. $P_N(z)$ is the depth profile of the nuclear polarization—the information we seek from PNR. We independently controlled the neutron and nuclear spin orientation to measure R_l^+ and R_l^- for left CPL incident on the sample, and R_r^+ and R_r^- for right CPL.

In order to assess the spin dependence of the neutron reflectivity, we define a quantity called the neutron spin asymmetry $A_i = (R_i^+ - R_i^-)/(R_i^+ + R_i^-)$, where the subscript i is either r or l . The neutron spin asymmetries A_r and A_l are shown for sample A in Fig. 3(a) as circle and open-cross-square symbols, respectively (dashed curves connect the symbols). Since P_N is reversed when the helicity of the CPL is reversed (Fig. 1), the relationship $R_r^\pm = R_l^\mp$ leads us to expect that $A_r = -A_l$ in the absence of instrumental (non-light-polarization-induced) effects. To show this relationship, the data in Fig. 3(a) are plotted in Fig. 3(b) as A_r vs A_l . The result of a

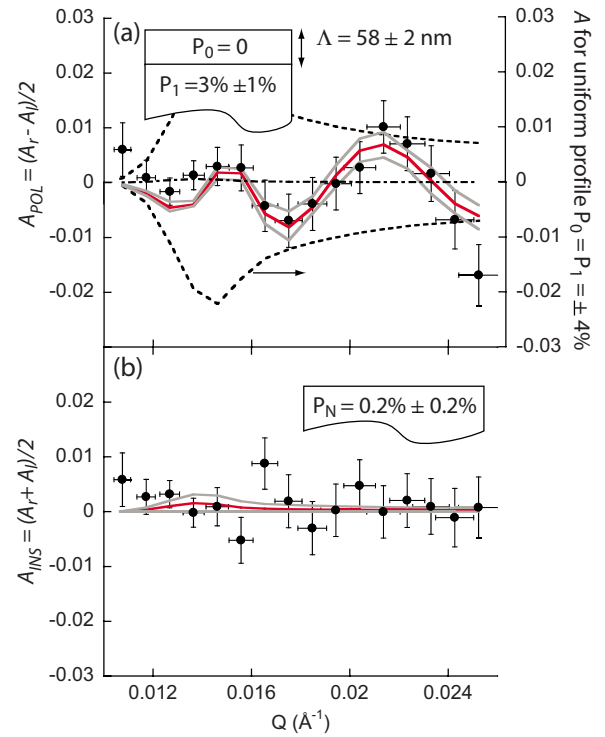


FIG. 4. (Color online) Neutron spin asymmetry for sample A corresponding to (a) nuclear polarization $A_{pol} = (A_r - A_l)/2$ and (b) instrumental effects $A_{ins} = (A_r + A_l)/2$. Inset: diagrams showing the nuclear polarization in GaAs for (a) nonuniform ($P_0 \neq P_1$) and (b) uniform models ($P_0 = P_1 = P_N$) yielding the red curves (gray curves obtained using the limits shown as uncertainties). The dashed (dot-dashed) curve is a calculation for $P_0 = P_1 = 4\%$ ($P_0 = P_1 \approx 0$).

principal component analysis²³ of the data in Fig. 3(b) is the solid line that minimizes the sum of the orthogonal distances between the solid line and the data (an example is the dashed line). This analysis treats symmetrically the errors in A_r and A_l . Since the slope of the line $\zeta_{r,l(A)} = -0.9 \pm 0.1$ is very close to -1 (the result for negatively related distributions), the data are compelling evidence that A_r is negatively related to A_l and that instrumental effects (which lead to positive slopes) are small. A principal component analysis comparing left and off data and right and off data for sample A yielded $\zeta_{l,off} = 0.36 \pm 0.23$ and $\zeta_{r,off} = -0.28 \pm 0.25$, respectively. The opposite signs are a consequence of comparing negatively related distributions, A_r and A_l , to a common distribution A_{off} . In contrast, a comparison of A_r and A_l for sample B yielded a *positive* value $\zeta_{r,l(B)} = +0.7 \pm 0.1$. A positive value means that A_r and A_l for sample B are not zero and are positively related as expected if the correlation is due to an instrumental effect. Notably, however, reversal of the helicity of CPL did not affect the neutron spin asymmetry for this sample—consistent for a sample having little or no nuclear polarization.

A_r and A_l contain components that are independent of and dependent on light polarization. $A_{ins} = (A_r + A_l)/2$ [Fig. 4(b)] is the (instrumental) part of the neutron spin asymmetry that is independent of light polarization since the effects of right and left CPL cancel each other in the average of the two

measurements. A_{ins} has a mean and standard deviation of 0.001 ± 0.003 for sample A [Fig. 4(b)] and 0.005 ± 0.006 for sample B (see Ref. 21). Thus, the instrumental contribution to the neutron spin asymmetry is approximately 1 part in 1000 for sample A and 1 part in 200 for sample B.²⁴ $A_{pol} = (A_r - A_l)/2$ [Fig. 4(a)] is the part of the neutron spin asymmetry that depends on light polarization (and hence P_N) since the influence of right and of left CPL reinforce each other (and the instrumental effects cancel each other).

The systematic variation of A_{pol} with Q is direct evidence for a nonuniform distribution of nuclear polarization with depth. The simplest representation of such a distribution consistent with $A_{pol}(Q)$ is to ascribe different neutron spin-dependent scattering lengths to the top and bottom parts of the sample [thus introducing a second interface (the first is the sample's surface), inset of Fig. 4(a)]. The change of the scattering length across the two interfaces gives rise to a modulation of $A(Q)$. $A(Q)$ can be analytically calculated for the case of one layer with thickness Λ (i.e., the separation between two interfaces) and nuclear polarization P_0 (representing the nuclear polarization near the surface of GaAs) on a second (infinitely thick) layer with nuclear polarization P_1 (representing the bulk nuclear polarization, see inset of Fig. 4). The result (correct to first order in P_0 and P_1) is given by Eq. (1), where N for GaAs is $0.022 \text{ f.u./\AA}^{-3}$.²⁵

$$A(Q) = \left(\frac{2I}{2I+1} \frac{\Delta b}{b_c} \right) \left(\frac{Q}{\sqrt{Q^2 - 16\pi N b_c \Lambda}} \right) \times [P_0 + (P_1 - P_0) \cos \sqrt{Q^2 - 16\pi N b_c \Lambda} \Lambda] \approx \left(\frac{2I}{2I+1} \frac{\Delta b}{b_c} \right) \times [P_0 + (P_1 - P_0) \cos Q \Lambda]. \quad (1)$$

The prefactor is small for GaAs $\sim 17\%$. The expression for $A(Q)$ is remarkable in that the three distinct characteristics of the Q -dependent neutron spin asymmetry—the period and amplitude of the oscillation and the mean—separately determine the magnitudes of Λ , P_1 , and P_0 for our model. The mean of $A_{pol} = (A_r - A_l)/2$ for sample A [Fig. 3(a)] is -0.0008 , so an upper bound on the net nuclear polarization near the surface of sample A is $|P_0| \sim 0.005$.

To obtain information about the depth dependence of nuclear polarization in sample A, we compare data in Fig. 4 to the neutron spin asymmetry calculated for cases where the nuclear polarization is uniform ($P_0 = P_1$) and nonuniform ($P_0 \neq P_1$). In order to account for the resolution of the instrument (which varies with Q , as shown by the horizontal error bars in Figs. 3 and 4), the spin-dependent neutron reflectivities $R^\pm(Q)$ were first calculated using the (dynamical) formalism of Parratt.²⁶ Next, the reflectivities were convoluted with instrumental resolution and then $A(Q)$ computed. The dashed curves in Fig. 4(a) show the $A(Q)$ anticipated for uniform nuclear polarization of $P_0 = P_1 = \pm 4\%$. The disagreement between the calculation and the neutron data rules out the possibility of uniform nuclear polarization with the value inferred from the Hanle curves.²⁷

On the other hand, the nonuniform model can explain why neutron scattering and the luminescence experiments obtain different results. Using $P_0 = 0$ (implied by the near zero mean of A_{pol}), we obtain $\Lambda = 58 \pm 2 \text{ nm}$ and $P_1 = 3\% \pm 1\%$ for a simple single layer model that best fits (by minimizing an error metric χ^2)²⁸ our neutron data (red curve, Fig. 4). Our model suggests that nuclear polarization exists in the sample bulk (as inferred from luminescence) but is suppressed near its surface.

We explored the sensitivity of P_1 and Λ to constraining $P_0 = 0$. Fits of the single layer model allowing P_0 to vary yielded an optimum value for P_0 that was not significantly different from zero. Nor did these fits produce any significant change in the amplitude of the oscillation $P_1 - P_0$, or its period Λ . We also examined the sensitivity of our model to the presence of a smeared nuclear polarization profile across the P_0/P_1 interface. $A(Q)$ was not significantly affected nor were the values of P_0 , P_1 , and Λ , for smeared nuclear polarization profiles that varied as an error function (typical for diffusion) with characteristic widths from 0 to 5 nm.

The nuclear spin diffusion length $\sqrt{DT_1}$ can be estimated using the spin diffusion constants for the isotopes in GaAs $D \sim 10^{-13} \text{ cm}^2/\text{s}$ (Refs. 29 and 30) and the nuclear spin relaxation time. For $T_1 = 1 - 10 \text{ s}$ (measured optically as described previously), the nuclear spin diffusion length $\sqrt{DT_1}$ is 3–10 nm, and its effect on our neutron data cannot be observed.

In order to further investigate the robustness of our analysis protocol, we applied it to neutron scattering data that should yield null results. We have three such “control” measurements. The first is a measurement of sample A with the light turned off.²¹ The second is $A_{ins} = (A_r + A_l)/2$ for sample A [Fig. 4(b)]. The third is $A_{pol} = (A_r - A_l)/2$ for sample B.²¹ For these cases, fits of the uniform model yielded $P_0 = P_1$ ranging from 0.1% to 0.6%. Fits of the nonuniform model $P_0 \neq P_1$ did not significantly improve the goodness-of-fit metric, so there is no evidence for depth-dependent nuclear polarization in these data.

IV. DISCUSSION

We suggest that two factors contribute to the suppression of nuclear polarization near the surface. First, since occupied donor sites are required for efficient DNP, nuclear polarization is not generated in the surface depletion region. The electric field at the surface of the sample is approximately 10^5 V/cm ,³¹ and given the binding energy (5.8 meV) (Ref. 32) and characteristic dimension of the electron wave function (9.9 nm),³² Si donor sites will not be occupied for electric fields greater than 5000 V/cm. Based on a self-consistent solution of the Poisson equation,³¹ this criterion yields an effective depletion depth of 30 nm for sample A.³³ The second contributing factor is the suppression of nuclear spin diffusion due to the relatively short nuclear spin relaxation time T_1 in our sample (at 20 K and 265 G). As noted above, we infer a nuclear spin diffusion length of 3–10 nm in our samples. As a result, nuclear polarization generated by efficient DNP in the bulk of the sample cannot diffuse to the surface. We also note that large electric field gradients near

the surface might further reduce T_1 , and hence the diffusion length, below the bulk value.

V. CONCLUSION

In summary, we have detected nuclear polarization of GaAs by measuring the scattering of polarized neutron beams. The wave vector dependence of the neutron spin asymmetry enables us to conclude that nuclear polarization is not uniform across the depth of the GaAs sample. A profile of nuclear polarization that is suppressed within ~ 60 nm of the GaAs surface and then increases to $\sim 3\%$ in the GaAs bulk explains the neutron data and is consistent with measurements of bulk nuclear polarization inferred from luminescence. The suppression of nuclear polarization near the GaAs surface is a probable consequence of the absence of DNP near the surface (due to unoccupied donor sites) and the relatively short nuclear spin diffusion length in compensated p -type GaAs that precludes diffusion of nuclear polarization into the surface region. Suppression of nuclear polarization near the GaAs surface (and by extension to any interface that is accompanied by a modest electric field) suggests that the influence of nuclear polarization on electron spin dynamics near the surface (or interface) should be minimal. The sensitivity of polarized neutron reflectometry to the very small

neutron spin dependence produced by nuclear polarization in GaAs was made possible by minimizing (e.g., through millisecond modulation of the neutron spin flipper) and canceling (e.g., by comparison of data taken with right and left circularly polarized light³⁴) instrumental sources of neutron spin asymmetry to about 1 part in 10^3 . Further advances in small signal detection may be possible in the future since efforts in the nuclear physics community³⁵ have demonstrated reductions of instrumental sources of neutron spin asymmetry to 1 part in 10^8 .

ACKNOWLEDGMENTS

We thank J. Kinney for technical assistance. Discussions with S. Crooker and D. L. Smith (LANL), W. Snow (Indiana), and A. McDowell (ABQMR, Inc.) are gratefully acknowledged. This work was supported by the Office of Basic Energy Science, U.S. Department of Energy, BES-DMS, and Laboratory Directed Research and Development program funds. Work at the University of Minnesota was supported by the NSF MRSEC program under Grant No. DMR 02-12302. T.K. acknowledges the support of JSPS. Neutron data were obtained at the Lujan Neutron Scattering Center at LANSCE, which is funded by the Department of Energy's Office of Basic Energy Science. Los Alamos National Laboratory is operated by Los Alamos National Security LLC.

*Present address: National Institute of Standards and Technology, Gaithersburg, MD 20899.

[†]On leave from Imaging Science and Engineering Laboratory, Tokyo Institute of Technology, Yokohama 226-8503, Japan.

¹S. Datta and B. Das, Appl. Phys. Lett. **56**, 665 (1990).

²G. Lampel, Phys. Rev. Lett. **20**, 491 (1968).

³R. R. Parsons, Phys. Rev. Lett. **23**, 1152 (1969).

⁴R. Fiederling, M. Keim, G. Reuscher, W. Ossau, G. Schmidt, A. Waag, and L. W. Molenkamp, Nature (London) **402**, 787 (1999).

⁵Y. Ohno, D. K. Young, B. Beschoten, F. Matsukara, H. Ohno, and D. D. Awschalom, Nature (London) **402**, 790 (1999).

⁶J. M. Kikkawa and D. D. Awschalom, Phys. Rev. Lett. **80**, 4313 (1998).

⁷S. W. Brown, T. A. Kennedy, D. Gammon, and E. S. Snow, Phys. Rev. B **54**, R17339 (1996).

⁸D. Paget, G. Lampel, B. Sapoval, and V. I. Safarov, Phys. Rev. B **15**, 5780 (1977).

⁹A. K. Paravastu and J. A. Reimer, Phys. Rev. B **71**, 045215 (2005).

¹⁰G. P. Felcher, R. O. Hilleke, R. K. Crawford, J. Haumann, R. Kleb, and G. Ostrowski, Rev. Sci. Instrum. **58**, 609 (1987).

¹¹C. F. Majkrzak, Physica B **221**, 342 (1996).

¹²M. R. Fitzsimmons and C. F. Majkrzak, in *Modern Techniques for Characterizing Magnetic Materials*, edited by Y. Zhu (Kluwer, Boston, 2005), pp. 107–152.

¹³M. D. Sturge, Phys. Rev. **127**, 768 (1962).

¹⁴The hyperfine field B_N is an effective field representing the interaction between an electron and a donor site. The hyperfine field

is not the dipolar field from a magnetic material.

¹⁵*Optical Orientation*, edited by F. Meier and B. P. Zakharchenya (North-Holland, Amsterdam, 1984).

¹⁶W. Hanle, Z. Phys. **30**, 93 (1924).

¹⁷V. G. Fleisher and I. A. Merkulov, in *Optical Orientation*, edited by F. Meier and B. P. Zakharchenya (North-Holland, Amsterdam, 1984), pp. 173–258.

¹⁸ $P_N = B_N/5.3$ T is derived from Eqs. (2)–(19) (Ref. 8).

¹⁹O. Schärpf, *Neutron Spin Echo*, edited by F. Mezei (Springer-Verlag, Berlin, 1980) pp. 35–39.

²⁰A Mezei π flipper consists of two coils. A steady current through one coil produces a magnetic field that cancels the static laboratory magnetic field \vec{B}_0 . Current through a second coil produces a magnetic field that is perpendicular to \vec{B}_0 , causing the neutron polarization to precess. By changing the magnitude of the current in this coil as a function of time, the field integral over time and distance inside the coil is tuned to assure that the spin of every neutron regardless of its wavelength reverses direction once the neutron exits the flipper.

²¹See EPAPS Document No. E-PRBMDO-76-030744 for data for samples A and B. For more information on EPAPS, see <http://www.aip.org/pubservs/epaps.html>.

²²*Neutron Data Booklet*, edited by A.-J. Dianoux and G. Lander (Institut Laue-Langevin, Grenoble, 2002).

²³K. Pearson, Philos. Mag. **2**, 559 (1901).

²⁴Improvements to the neutron instrument months reduced A_{ins} for sample A.

²⁵ $A(Q)$ was obtained by solving Schrödinger's equation for our model and is valid for $Q > \sqrt{16\pi N b_c} = 0.012 \text{ \AA}^{-1}$. For smaller Q , $A(Q)$ is zero.

- ²⁶L. G. Parratt, Phys. Rev. **95**, 359 (1954).
- ²⁷No evidence for a large uniform nuclear polarization in a related GaAs sample was obtained with PNR at the NIST Center for Neutron Research.
- ²⁸P. R. Bevington and D. K. Robinson, *Data Reduction and Error Analysis for the Physical Sciences*, 3rd. (McGraw-Hill, Boston, MA, 2003), p. 67.
- ²⁹D. Paget, Phys. Rev. B **25**, 4444 (1982).
- ³⁰J. Lu, M. J. R. Hoch, P. L. Kuhns, W. G. Moulton, Z. Gan, and A. P. Reyes, Phys. Rev. B **74**, 125208 (2006).
- ³¹SIMWINDOWS, Version 1.5.0, Copyright ©1994, 1999 by David W. Winston. The Fermi level was assumed to be pinned close to midgap at the surface.
- ³²P. Lane and R. L. Greene, Phys. Rev. B **33**, 5871 (1986).
- ³³120 nm for sample B.
- ³⁴We were able to detect nuclear polarization in our sample by comparing the difference between neutron scattering signals after the direction of the nuclear polarization was reversed. Similarly, detection of pinned magnetic spins at the interface between ferromagnetic and antiferromagnetic materials was achieved by comparing the neutron reflectivities before and after reversal of a magnetic field. See, for example, M. R. Fitzsimmons B. J. Kirby, S. Roy, Z. P. Li, V. Roshchin, S. K. Sinha, and I. K. Schuller, Phys. Rev. B **75**, 214412 (2007).
- ³⁵M. T. Gericke, J. D. Bowman, R. D. Carlini, T. E. Chupp, K. P. Coulter, M. Dabaghyan, M. Dawkins, D. Desai, S. J. Freedman, T. R. Gentile *et al.*, Phys. Rev. C **74**, 065503 (2006).